ORIGINAL ARTICLE

Concentration distribution, enrichment and controlling factors of metals in Al-Shuaiba Lagoon sediments, Eastern Red Sea, Saudi Arabia

Ramadan H. Abu-Zied[1,4] · Bandar A. Al-Mur[2] · Mohammed I. Orif[1] · Ahmed Al Otaibi[3] · Mohammed A. Ghandourah[1]

Abstract

Fifty surficial bottom sediments from the Al-Shuaiba Lagoon (80 km south of Jeddah City, eastern Red Sea, Saudi Arabia) were investigated for some major and trace metals to map their concentration distribution in the lagoon, shed light on their origin and controlling factors, and to establish potential risks to living organisms through comparison with sediment quality guidelines (SQGs). Statistical analyses allowed the division of metals into five associations: (1) Mg-Ca-Sr, (2) Al-Zn-Cr-Ni-Cu, (3) Fe–Mn-Li, (4) K and (4) Pb–Cd. Their distributions indicated that elevated values of Al, Mg, Fe, Sr, K, Mn, Li, Zn, Cr, Cu, Pb, Ni and Cd occurred in high intertidal areas and in mangrove sediments. These decreased gradually towards the deeper waters and inlet, except for Ca, which had its highest concentration in the centre of the lagoon. Major elements mainly appear to originate from the mineralization and evaporation of the lagoon's water, whereas trace elements appear to originate from wind-blown dust and runoff, with subsequent concentration in sediments aided by adsorption onto fine particles and organic carbon complexes. Enrichment indices and a pollution load index (PLI) indicated that the lagoon sediments were highly enriched with Sr, Pb and Cd, with the latter two and PLI being the highest at the eastern side of the lagoon. Comparison with the SQGs showed that the concentrations of Cu, Pb and Cd are higher than the effect range low (ERL) and threshold effect level (TEL), but are lower than the effect range median (ERM). This suggests that these metals might cause an occasional threat to the biota in the eastern part of the lagoon.

Keywords Lagoon · Metals · SQGs · Redox conditions · Enrichment · Mangroves

Introduction

Concentrations of heavy metals in the coastal marine sediments and their bioavailability in the overlying waters have gained a lot of attentions not only due to the danger

associated with them, especially when they occur with elevated values in reducing conditions, but also due to their environmental persistence, non-degradability and eco-toxicological risks through transfer into the food chain (Sakan et al. 2006; Sarkar 2018). The heavy metals have a specific gravity > 5 g/cm3 and some of them, such as Fe, Mn, Zn, Cu and Ni, are considered as essential micronutrients necessary for a healthy biota growth (Zhuang et al. 2009; Tiwari and Lata 2018; Almahasheer et al. 2018). In the open seawaters and at the mouths of rivers, their bioavailability boosts the primary productivity in the ocean (Martin et al. 1990; Poulton and Raiswell 2002; Wehrmann et al. 2014). When the concentrations of such metals exceed the permissible limit, they become toxic affecting the consumers and consequently increase the environmental health risks (Nagajyoti et al. 2010; Kumar et al. 2016; Tiwari and Lata 2018). The heavy metals, such as Pb, Cd, and Cr, are non-essential and considered highly toxic (Kumar et al. 2016; Tiwari and Lata

✉ Ramadan H. Abu-Zied
  rabuzied@kau.edu.sa

[1] Marine Chemistry Department, Faculty of Marine Sciences, King Abdulaziz University, P.O. Box 80207, Jeddah 21589, Saudi Arabia

[2] Department of Environmental Sciences, Faculty of Meteorology, Environment and Arid Land Agriculture, King Abdulaziz University, Jeddah 21589, Saudi Arabia

[3] Department of Chemistry, Faculty of Science, University of Hail, Hail 81451, Saudi Arabia

[4] Geology Department, Faculty of Science, Mansoura University, El-Mansoura 35516, Egypt

2018; Sarkar 2018; Almahasheer et al. 2018). The mobility and bioavailability of the above-mentioned metals in pore waters/sediments and the overlying waters depend on the interplay of many parameters, such as sediment grain size, pH, dissolved oxygen, salinity, redox potential, iron-manganese (oxyhydr)oxides, organic carbon and living organisms (Souza et al. 2015; Hariri and Abu-Zied 2018; Sarkar 2018). Moreover, their bioaccumulation in the biota has been noticed and may pose a threat to consumers (e.g., Esmaeilzadeh et al. 2016; Maurya and Malik 2019) or to the primary producers themselves (e.g., Usman et al. 2013; Almahasheer et al. 2018).

The metals Mg, Ca, K and Sr are also essential macro-elements for shell secretion of calcareous organisms and bone productions (Simionov et al. 2019). The concentrations of major metals, such as Mg, Ca, K, Sr and Al, in sediments of coastal marine settings are commonly used to distinguish between the marine and terrestrial influences. For example, high Mg and Sr in carbonates are markers for strong evaporation as in hypersaline lagoons. Also, Al is an index of fine-grained aluminosilicate detritus, so it is widely used as a normalizer because it is not affected by the anthropogenic activities (Badr et al. 2009; Garcia et al. 2009). Their ratios, such as Mg/Ca, Sr/Ca and Mg/Sr, in skeletal carbonates are extensively used as proxies for paleotemperature (Tripati et al. 2003; Tang et al. 2012). Also, the ratios of Fe/Ca and Mn/Ca are considered as potential proxies for redox conditions (Glock et al. 2012) and terrigenous inputs (Mulitza et al. 2007).

The concentrations of major and trace metals of the eastern Red Sea coastal sediments and its associated lagoons, khors, sharms and bays were investigated by many scholars to know the quantity of heavy metals in the studied sediments and use them as a base-line for future monitoring. For example, Badr et al. (2009) studied the metals in sediment cores collected from shallow depths off three major industrialized cities, such as Jeddah, Rabigh and Yanbu. They concluded that elevated concentrations of Pb were recorded in the core sediments off Jeddah due to use of gasoline; and Jeddah is the most polluted area, followed by Rabigh while Yanbu is the least contaminated area. Also, Al-Mur et al. (2017) have indicated the same conditions for the sediments of Jeddah's coast, where heavy metal concentrations in core sediments are increased near central Jeddah and have become higher in recent years due to contaminations by anthropogenic inputs. As a result of these anthropogenic inputs, some parts of Jeddah's coastal waters became enriched by heavy metals (Cu, Zn, Cd, Ni, Cr and Pb) and sludge (organic-rich sediments) creating many dead zones in these localities, where organic-rich and soft substrates dwellers have overcome and replaced the reefal organisms (Abu-Zied et al. 2013, 2016; Abu-Zied and Hariri 2016; Abu-Zied and Orif 2019).

Coastal lagoons, situated at the interface of land and sea, are generally shallow water bodies having limited exchange with sea, and support high biological productivity and rich biodiversity (Amir et al. 2019, 2020). The bottom sediments of the eastern Red Sea coastal lagoons, such as Al-Kharrar (Khor Al-Kharrar), Salman Bay (formerly called Ras Hatiba), Al-Shuaiba, and Al-Mejarma, were investigated with respect to heavy metals, which are mostly originated from the biogenic remains and terrestrial influx with no imprint of pollution sources (Basaham et al. 2015, 2019; Youssef and El-Sorogy 2016; Hariri and Abu-Zied 2018). However, Youssef and El-Sorogy (2016) concluded that the bottom sediments of the Al-Kharrar Lagoon had elevated concentrations of Pb and Cd that exceeded the environmental background values and sediments classified into non-polluted to heavily polluted with Pb, non-polluted to moderately polluted with Cu, and non-polluted with Mn, Zn, Cd, and Cr.

The Al-Shuaiba Lagoon (ASL) has a wealth of primary producers, such as mangroves, sea-grasses, macro-algae and unique faunal groups (Abu-Zied et al. 2011), so it is very attractive for many visitors and planners. The present environmental conditions and benthic foraminifera of the ASL were investigated by Abu-Zied et al. (2011) and Abu-Zied and Bantan (2013). They concluded that the lagoon is a hypersaline basin with highest salinity and temperature of 60% and 33 °C, respectively. This allowed proliferation of unique benthic foraminiferal assemblages in the bottom sediments of the lagoon. Only two studies were carried out on the concentrations of metals in the ASL (Abohassan 2013; Basaham et al. 2019). Basaham et al. (2019) investigated the elemental composition of sediments from the centre and inlet of ASL and concluded that the siliciclastic elements were related to terrigenous influx mainly by aeolian transportation, whereas carbonate-related elements were mainly of biogenic origin of calcareous skeletal remains. Abohassan (2013) concluded that the mangrove sediments were the main stocks for heavy metals in the ASL followed by mangrove woods and a minimal amount (< 3.5%) of heavy metals was returned back to the sediment via litter fall out of which, less than 1% was removed away from the mangrove system via tidal activities. Therefore, this study aims to determine the concentrations and spatial distributions of some major and trace metals in the bottom sediments of the whole area of the ASL and its inlet. More light will be shed on the controlling parameters that affect the metal quantities and distributions in the ASL sediments. Moreover, metals enrichments will be assessed using indices, such as enrichment factor (EF), contamination factor (CF), geo-accumulation index (Igeo) and pollution load index (PLI). The consensus-based sediment quality guidelines (SQGs) are employed to determine the extent of metals' toxicity on the lagoon's organisms.

The study area

The Al-Shuaiba Lagoon (ASL), often called "Al-Shuaiba Al-Kabirah", is located 80 km south of Jeddah City (Saudi Arabia) on the eastern Red Sea coast between latitudes 20° 42′ to 20° 51′ N and longitudes 39° 26′ to 39° 32′ E (Fig. 1). It is one of the Red Sea coastal lagoons that break the continuity of the Pleistocene reefal limestone terraces of elevation between 1 and 3 m a.s.l (Abu-Zied et al. 2011). These Pleistocene terraces separate the western side of ASL from the Red Sea, except at a very narrow inlet (about 60 m wide and 6 m deep) permitting two water layers to pass through (Abu-Zied et al. 2011). In the east, a very low-land borders the ASL and allows the tidal waters (0.25 m) to run over a wide area (Fig. 1).

Mangrove trees cover about 10% of the total areas of the ASL (Fig. 1), whereas the seagrasses and macro-algae (and filamentous green algae) dominate the rest of the lagoon substrates (Abu-Zied et al. 2011). The bottom sediment of the ASL is mainly composed of bioclastic grains, such as small molluscs, shell fragments, benthic foraminifera, coralline algal remains, pellets and lime mud (Abu-Zied and Bantan 2013, 2015).

The ASL has hypersaline waters with a maximum salinity and temperature of 56% and 33 °C at the shallow intertidal parts, then these values decrease to 38% and 29 °C at the inlet, respectively (Abu-Zied et al. 2011). The lagoon gained these conditions because it is a small and shallow
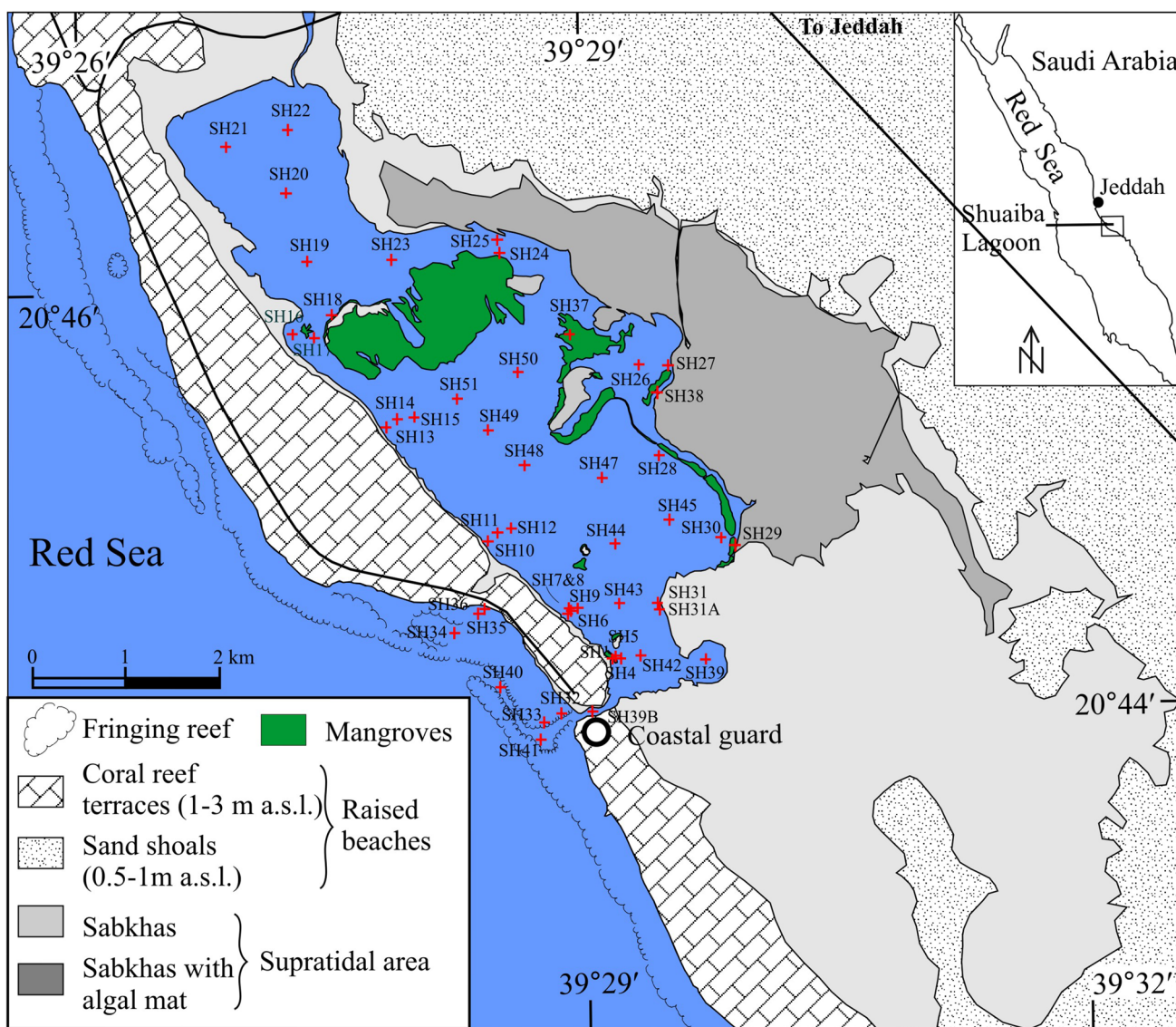

Fig. 1 Location map of Al-Shuaiba Lagoon, eastern Red Sea, showing the sample sites as crosses, modified after Abu-Zied and Bantan (2013)

basin (maximum water depth of 3 m), occurring under arid warm climate with scarce rainfall (63 mm/yr) and no riverine influx (Abu-Zied and Bantan 2015). The lagoon surface water's pH was the highest (8.5) at the inlet and the southern part of the lagoon, whereas at the intertidal area dominated by mangrove tress, it decreased to 8.2 (Abu-Zied et al. 2011).

Materials and methods

Sediment collection

Fifty surficial bottom sediment samples were used in this study (Fig. 1). Details on sample locations and coordinates were listed in Abu-Zied et al. (2011), see also Supplementary Information SI-1. These samples were collected from the upper 1 cm of the bottom sediments of the ASL during May–June 2010 using a knife when water depth is less than 1 m and on board by the Van Veen grab sampler at deeper waters, then stored in polyethylene jars. In the laboratory, all samples dried in an oven at 50 °C for 24 h and archived for further analysis, see Abu-Zied and Bantan (2013) for more details about this.

The environmental parameters (measured at each sample site) used in this study, such as water depth, pH, salinity, temperature, organic carbon (LOI) and sediment grain sizes as gravel, sand and mud, were taken from Abu-Zied et al. (2011) and Abu-Zied and Bantan (2013). The pH, salinity, temperature and DO were measured for the waters of the ASL and since this lagoon is very shallow, these parameters seem affecting the underlying sediments. These parameters are also listed in the Supplementary Information SI-1.

Elemental analysis

Aliquots of the sediment samples were dried at 100 °C for 24 h to remove waters, then ground using an agate pestle and mortar. Accurately weighed 0.2 g of each sample was digested with hot concentrated nitric acid under reflux for 24 h. This is because the studied sediments are mainly composed of carbonate-rich materials with rare lithogenous particles (Abu-Zied and Bantan 2015), which dissolve easily using HNO_3 (Rodger and Davies 1992; Clemente et al. 2008). For more details about the methodology see Abu-Zied et al. (2013) and Abu-Zied and Hariri (2016). Digested samples (solutions) were then evaporated to near dryness and diluted to constant volume (25 ml) with 10% HCl. After that, the concentrations of Al, Mg, Ca, Fe, Sr, K, Mn, Li, Zn, Cr, Cu, Pb, Ni and Cd were measured using Inductively Coupled Plasma-Optical Emission Spectrometer (ICP-OES) available at Faculty of Meteorology, Environment and Arid Land Agriculture, King Abdulaziz University. The

measurements were carried out by ICP-OES after calibration against standard curves of 100 ml of multi-element standard solution (766,333.1208, Applichem Panreac) with accuracy higher than 96.5%. The detection limits for the measured elements (µg/L) as follows: 3 (Al), 0.1 (Mg), 0.02 (Ca), 2 (Fe), 0.06 (Sr), 20 (K), 0.4 (Mn), 0.3 (Li), 1 (Zn), 2 (Cr), 0.4 (Cu), 10 (Pb), 5 (Ni), and 1 (Cd). To ensure best quality control and avoid cross-contamination, the glasswares were rinsed three times with diluted acid (Merck Suprapur grade) and last time with deionized water. The concentrations of the measured elements are presented in the supplementary information SI-1 and in graphs as mg/kg of bulk dry weight sediments.

Statistical analysis

Three approaches were used in this study, such as Pearson's correlation coefficients (r), the principal component (PCA) and factor analyses (FA). The matrix of the Pearson's correlation coefficients (r) was constructed by Excel 2013, whereas the PCA and FA were performed using the Past software (Hammer et al. 2001). The PCA is a correlation matrix, which normalizes all the studied variables; components 1 and 2 explained 38.5 and 10.5% of the total data variability, respectively (Fig. 2). In the FA, factors 1 and 2 explained 67.4 and 16% of the studied variables (Fig. 2).

Enrichment/pollution indices: In this study, many indices were employed, such as the enrichment factor (EF), contamination factor (CF), geo-accumulation index (Igeo) and pollution load index (PLI). This is because the enrichment of metals in the surficial sediments of the ASL whether from natural or anthropogenic processes cannot be determined by the metal concentrations alone. The derivation of these indices, in essence, was achieved by comparing the measured metal concentrations against the natural background of world average shale (Turekian and Wedepohl 1961) and normalizing by Al (Thomson et al. 2001; Badr et al. 2009; Diop et al. 2015). Al is used as a normalizer in this study instead of Fe and Li, because Al showed direct positive relationships with most of the studied metals, see Table 1. Also, Al is the main component of the fine-grained aluminosilicates and its concentrations are not influenced by the anthropogenic inputs (Garcia et al. 2009).

The EFs of elements were calculated using this equation: $EF = (M/Al)_{sample}/(M/Al)_{background}$ (Sutherland 2000), where $(M/Al)_{sample}$ denotes to the measured concentration of an element in the studied sample divided by Al of the same sample, and $(M/Al)_{background}$ denotes to the concentration of an element and Al in the world average shale (Turekian and Wedepohl 1961). The EF values have been categorized into five classes, such as low level enrichment from natural origin (EF < 2), moderate enrichment ($2 \leq EF < 5$), significant enrichment ($5 \leq EF < 20$), very high enrichment

Fig. 2 Scatter plots of A, the correlation-based principal component (PCA) and B, factor analyses (FA). Environmental parameters, such as sediment grain sizes (mud, sand and gravel fractions), organic carbon (LOI), depth, temperature, salinity and pH, were taken from Abu-Zied et al. (2011) and Abu-Zied and Bantan (2013). Dissolved oxygen (DO) is only presented here but it was measured during the same field work of the above parameters
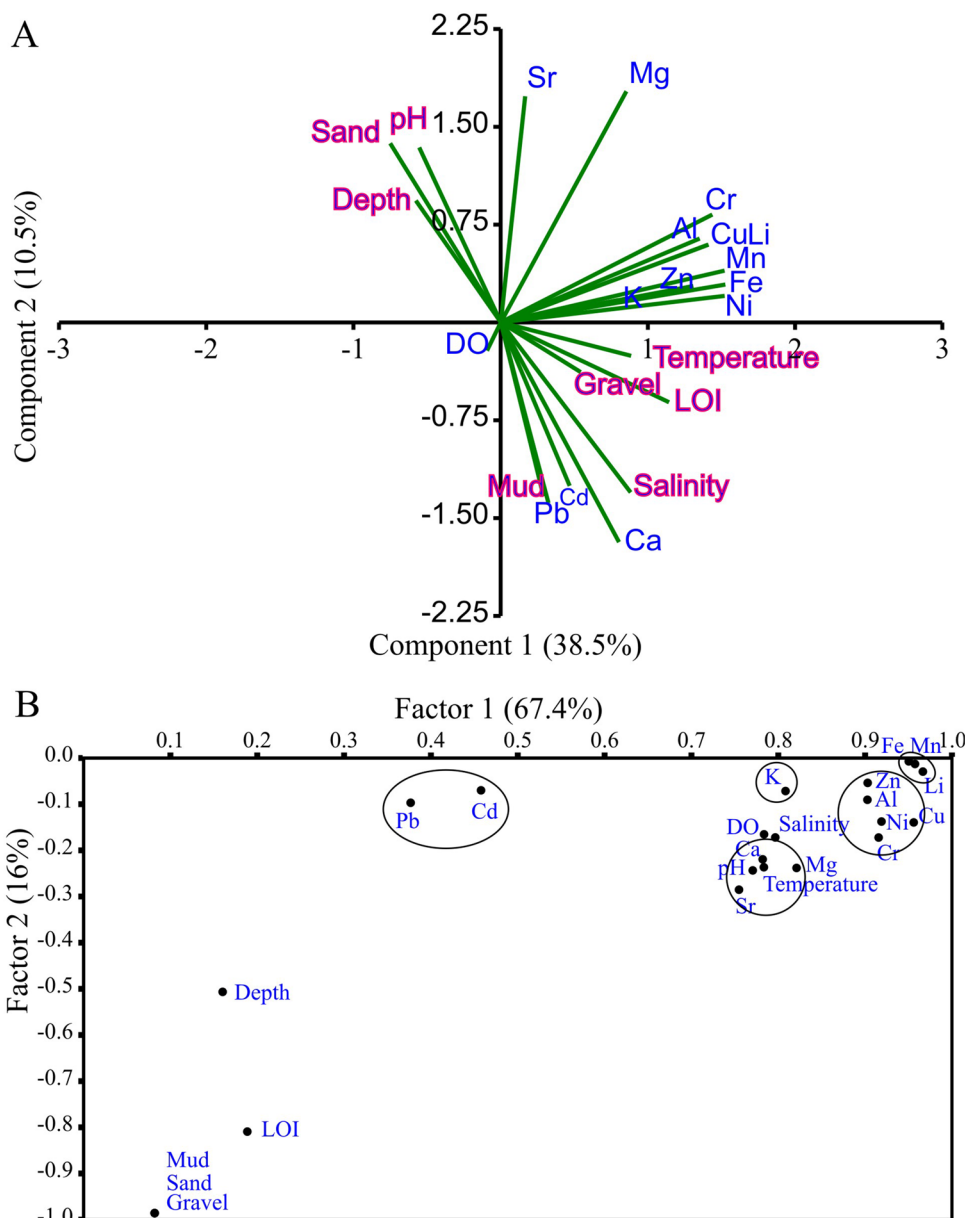
$(20 \leq EF < 40)$ and extremely high enrichment $(EF > 40)$ (Sutherland 2000).

The CF was also calculated based on the background of world average shale (Turekian and Wedepohl 1961), using this equation: $CF = M_{sample}/M_{background}$. When $CF < 1$, it indicates low level of contamination, the value of $1 \leq CF < 3$ indicates normal level of contamination, the value of $3 \leq CF < 6$ denotes to a considerable level of contamination and excessive level of contamination is indicated when $CF > 6$ (Hakanson 1980).

The Igeo Index was calculated using this equation $Igeo = \log 2 (Cn/(1.5 \times Bn))$. The Cn is the measured concentration of metal (n), and Bn the metal's concentration in the average shale (Turekian and Wedepohl 1961). It

separates sediments quality into different classes: unpolluted $(Igeo < 0)$, unpolluted to moderately polluted $(0 \leq Igeo < 1)$, moderately polluted $(1 \leq Igeo < 2)$, moderately to heavily polluted $(2 \leq Igeo < 3)$, heavily polluted $(3 \leq Igeo < 4)$, heavily to extremely polluted $(4 \leq Igeo < 5)$ and extremely polluted $(Igeo > 5)$ (Muller 1969; Hu et al. 2019).

The PLI was calculated using this equation: $PLI = (CF1 \times CF2 \times CF3 ... CFn)^{(1/n)}$. When PLI value > 1 indicates sediments are polluted whereas when it is < 1 indicates no pollution (Chakravarty and Patgiri 2009). The sediment quality guidelines (SQGs) used in this study are following those of Long et al. (1995) and MacDonald et al. (2000).

Table 1 Pearson correlation coefficients (r) between the environmental parameters such as water depth, pH, salinity, temperature, dissolved oxygen (DO), organic carbon (LOI) and sediment grain size (sand, gravel and mud), and the metals Al, Mg, Ca, Fe, Sr, K, Mn, Li, Zn, Cr, Cu, Pb, Ni and Cd

	Depth	pH	Salinity	Temp.	DO	LOI	Sand	Gravel	Mud	Al	Mg	Ca	Fe	Sr	K	Mn	Li	Zn	Cr	Cu	Pb	Ni	Cd
Depth	1																						
pH	0.31	1																					
Salinity	−0.44	−**0.66**	1																				
Temp.	−0.37	−0.30	0.35	1																			
DO	0.17	0.23	0.10	0.46	1																		
LOI	−0.35	−0.32	**0.70**	0.49	0.34	1																	
Sand	0.20	0.16	−0.19	−0.25	−0.21	−**0.56**	1																
Gravel	−0.13	−0.14	0.24	0.27	0.48	0.28	−0.44	1															
Mud	−0.13	−0.08	0.05	0.10	0.10	0.42	−**0.81**	−0.18	1														
Al	−0.25	−0.23	0.38	**0.50**	−**0.52**	0.56	−0.32	0.22	0.20	1													
Mg	−0.03	0.02	0.07	0.27	0.12	0.27	−0.10	0.25	−0.05	**0.55**	1												
Ca	−0.35	−0.24	0.37	0.20	−0.14	0.39	−0.44	0.02	0.47	0.24	−0.03	1											
Fe	−0.36	−0.37	**0.55**	0.45	−0.23	**0.70**	−0.36	0.19	0.27	**0.84**	**0.55**	0.44	1										
Sr	0.09	−0.02	0.06	0.18	0.04	0.13	0.08	0.13	−0.17	0.36	**0.50**	−**0.66**	0.14	1									
K	−0.23	−0.07	0.16	0.16	−0.08	0.40	−0.34	0.36	0.13	0.36	0.28	0.29	0.38	0.05	1								
Mn	−0.33	−0.33	**0.51**	0.42	−0.14	**0.65**	−0.32	0.32	0.15	**0.81**	**0.53**	0.45	**0.95**	0.11	0.45	1							
Li	−0.25	−0.09	0.29	0.35	−0.34	**0.55**	−0.28	0.14	0.21	**0.64**	0.42	0.43	**0.83**	−0.05	0.41	**0.84**	1						
Zn	−0.13	−0.16	0.33	0.34	−0.34	**0.54**	−0.23	0.25	0.09	**0.65**	0.30	0.37	**0.69**	−0.01	0.39	**0.73**	**0.83**	1					
Cr	−0.15	−0.15	0.26	0.42	0.01	**0.53**	−0.33	0.23	0.21	**0.80**	**0.64**	0.29	**0.86**	0.20	0.39	**0.86**	**0.80**	**0.70**	1				
Cu	−0.16	−0.07	0.23	0.37	−0.16	**0.58**	−0.32	0.23	0.20	**0.65**	0.43	0.40	**0.77**	−0.02	0.40	**0.81**	**0.96**	**0.87**	**0.83**	1			
Pb	−0.04	−0.21	0.26	0.16	**0.88**	0.12	−0.19	0.38	−0.05	0.15	−0.02	0.04	0.07	0.07	−0.02	0.07	−0.02	**0.23**	0.13	0.05	1		
Ni	−0.31	−0.29	0.48	0.46	−0.10	**0.68**	−0.41	0.27	0.27	**0.71**	**0.51**	0.45	**0.88**	0.04	0.42	**0.88**	**0.87**	**0.72**	**0.88**	**0.87**	0.07	1	
Cd	−0.08	−0.16	0.23	0.12	0.21	0.16	−0.19	0.29	0.02	0.21	−0.04	0.13	0.11	0.03	−0.04	0.08	0.00	0.21	0.18	0.06	**0.79**	0.11	1

Results and discussion

Metals spatial distributions and their relationships with the environmental parameters

The best grouping of metals in the sediments of ASL is reconstructed by their distributional patterns and using three approaches, which are Pearson's correlation coefficient (r) and the scatter plots of the principal component (PCA) and factor analyses (FA). These techniques allowed the division of metals into five associations: (1) Mg-Ca-Sr, (2) Al-Zn-Cr-Ni-Cu, (3) Fe–Mn-Li, (4) K and (4) Pb–Cd (Fig. 2).

The association Mg-Ca-Sr: It is made of major elements that predominate in warm shallow tropical environments, showing concentrations with averages of $13{,}546 \pm 3032$, $10{,}112 \pm 376$, and 3986 ± 1022 mg/kg of bulk sediments, respectively (Fig. 3). These elements could have originated from the lagoon's water mineralization during evaporation concentration of the lagoon's waters and precipitation of biogenic and non-skeletal carbonates. Ca concentration in the studied sediments showed lower values than those of the Red Sea coast (Table 2). This association showed a close affinity to pH, temperature, salinity and DO as indicated by the plot of FA (Fig. 2). However, they showed no affinity to the water depth, organic carbon (LOI) and sediment grain sizes (Fig. 2). Such relationships are not or very weakly developed in the correlation matrix (Table 1) and in the plot of PCA (Fig. 2). In the plot of PCA, Ca is strongly positively correlated with Pb, Cd, mud and salinity; it is strongly inversely correlated with Mg, Sr, pH, sand, and water depth (Fig. 2). The Mg and Sr showed their maximum values in the sediments of supra-, and inter-tidal areas that are characterized by the highest temperature and salinity of 33 °C and > 52% (Abu-Zied et al. 2011), whereas their low values were recorded in the centre of the ASL (Fig. 3). On the contrary, the highest values of Ca occurred in the centre of the ASL and its low values were recorded in the supra-, and inter-tidal areas (Fig. 3). This is probably related to occurrence of high temperature and salinity in these areas allowing precipitation of high Sr-Mg-carbonates in forms of aragonite and calcite (Ries 2010), and additionally incorporation of Mg promotes the precipitation of Sr (Weinbauer and Velimirov 1995).

In the Red Sea's lagoons, aragonite is the dominant mineral, representing about 40% of the total bulk sediments whereas the calcite and dolomite represent values of 13 and 23%, respectively (Bantan and Abu-Zied 2014). It is also reported that aragonite and high-Mg calcite are the dominant carbonate phases in warm tropical to subtropical waters (Stanienda-Pilecki 2018; Basaham et al. 2019). This may explain why the intertidal area of ASL contains the highest concentrations of Mg and Sr. Similar testifying results were also reported by many authors. For example, Sunagawa et al. (2007) indicated that increasing temperature promotes the precipitation of aragonite (not calcite), which is enriched in Sr. On the other hand, Weinbauer et al. (2000) indicated that temperature promotes the incorporation of Mg in biogenic calcite whereas the Sr concentration is inversely related to the growth rate and consequently the concentrations of Mg and Sr in some organisms could be used as ecological indicator for temperature and growth rate. Tang et al. (2012) discussed that non-lattice sites were probably related to site defects with preferential incorporation of larger cations such as Sr^{2+} than Ca^{2+}, especially during fast precipitation that resulted in more Sr partitioning into calcite. However, many studies reported that salinity has no effect on the incorporation of Sr and Mg into the calcite lattice (Rosales et al. 2004; Gussone et al. 2010). Tang et al. (2012) also concluded that the discrimination of Sr^{2+} versus Ca^{2+} during calcite formation is mainly controlled by precipitation rate and is weakly influenced by ionic strength or salinity. Toler et al. (2001) also mentioned that biogenic high-Mg calcite tends to be particularly abundant in shallow tropical carbonate reefs and shelf environments, where seawaters are supersaturated with respect to $CaCO_3$ and thermodynamically favors the precipitation of high-Mg calcite or aragonite crystals.

The association K: It showed concentration with an average of 2137 ± 1904 mg/kg of bulk sediments (Fig. 3). The maximum values were recorded in the sediments of supra-, and inter-tidal areas of the ASL where temperature and salinity increased to 33 °C and > 52% (Abu-Zied et al. 2011); its low values were recorded in the sediments of the inlet and southern part of the lagoon (Fig. 3). It shows, more or less a gradient in its concentration increasing from south (inlet) to the upper part of the lagoon following the surface water salinity (see Abu-Zied et al. 2011). It is displayed alone in the scatter plot of FA, showing no close affinity with the environmental parameters, such as the water depth, LOI and sediment grain sizes (Fig. 2). This is in agreement with those of the Pearson's correlation matrix (Table 1). In the plot of PCA, the K is strongly positively correlated with the Al, Zn, Cr, Ni, Cu, Fe, Mn and Li; and it is weakly correlated with temperature, gravel and organic carbon (Fig. 2). The K in the ASL sediments is possibly originated from the lagoon's waters mineralization as a result of high evaporation and precipitation of salts and carbonates. The wind-blown dust could also contains K-rich clay minerals.

The association Al-Zn-Cr-Ni-Cu: It showed concentrations with averages of $30{,}180 \pm 20{,}392$, 70 ± 65, 41 ± 19, 16 ± 6 and 40 ± 28 mg/kg of bulk sediments, respectively (Figs. 3 and 4). This association showed their maximum values in the northern and eastern sides of the lagoon
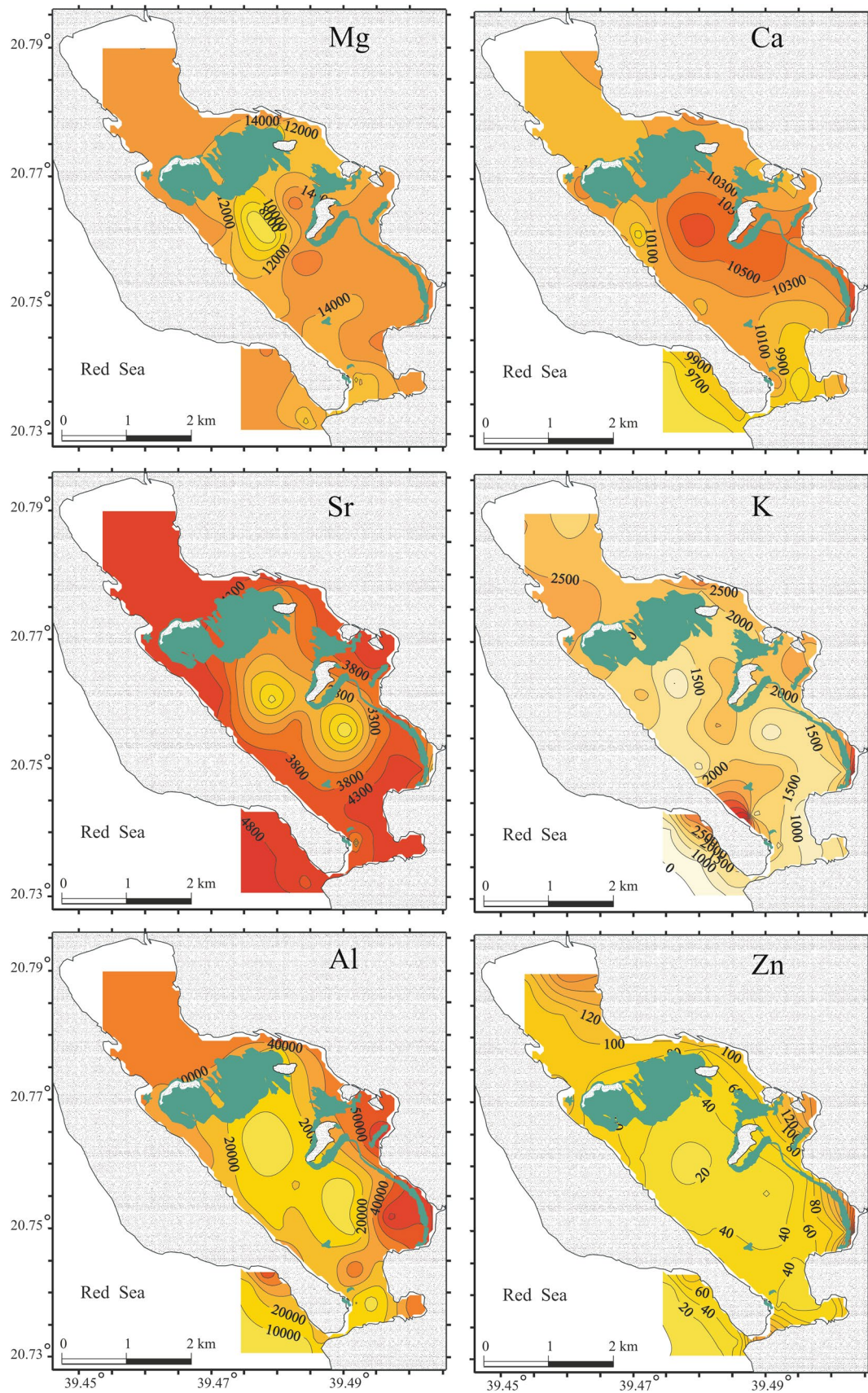
Fig. 3 Concentration (mg/kg) distribution of the metals Mg, Ca, Sr, K, Al and Zn in the surficial bottom sediments of Al-Shuaiba Lagoon

Table 2 Enrichment factor (EF), contamination factor (CF), geo-accumulation index (Igeo) and comparison of average concentrations (mg/kg) of metals Al, Mg, Ca, Fe, Sr, K, Mn, Li, Zn, Cr, Cu, Pb, Ni and Cd measured in the surficial bottom sediments of Al-Shuaiba Lagoon (this study) with those of the Red Sea, worldwide and SQGs

Location		Al	Mg	Ca	Fe	Sr	K	Mn	Li	Zn	Cr	Cu	Pb	Ni	Cd	Reference
Al-Shuaiba Lagoon (this study)	Min.	274	4267	9396	358	760	352	6	0	3	3	3	2	6	0	This study
	Max.	75116	17483	11357	14067	4813	12277	297	496	396	119	204	272	42	9	
	St. Dev.	20392	3032	376	2939	1022	1904	56	75	65	19	28	49	6	2	
	Average	30180	13546	10112	4899	3986	2137	91	79	70	41	40	37	16	1.58	
	EF	1.00	11.2	7.67	0.55	102.5	0.64	0.58	4.49	3.94	2.41	4.99	13	2.30	42.5	
	CF	0.38	0.90	0.46	0.10	13.3	0.08	0.11	1.19	0.73	0.46	0.88	1.83	0.23	5.28	
	Igeo	−0.79	−0.24	−0.51	−1.28	0.92	−1.38	−1.25	−0.23	−0.46	−0.58	−0.31	−0.14	−0.85	0.32	
Red Sea lagoons:																
Shuaiba Lagoon			10921 (5356–18909)		8752 (34–28052)		1213 (548–3774)	106 (54–203)		11 (0–51)	14 (0–44)	6 (1–18)		19 (14–29)		Abu-Zied and Bantan (2015)
Shuaiba Lagoon		25139	34312	423746	16800	5581	2823	310		30.6	41.7	31.9		15.4		Basaham et al. (2019)
Al-Kharrar Lagoon					18734 ±11202			329±143		23.6±16		22.4±12	0.05±0.25	26.9±17	0.31±1.6	Hariri and Abu-Zied (2018)
Al-Kharrar Lagoon					2249 (1708–3686)			103 (53–225)		40 (30–51)	20.62 (14–25)	16 (11–28)	51 (40–63)	9 (8–10)	0.26 (0.188–0.33)	Youssef and El-Sorogy (2016)
Sharm Obhur (Zone A)		55000	28000	140000	44000	1550		675		82	135	47	4.5	57		Ghandour et al. (2014)
Al-Arbaeen and Al-Shabab					14900			151		132	63.4	59.8	55.9	52.8	0.68	Abu-Zied et al. (2013)
Red Sea coast:																
Red Sea Coast			19200 (4500–95600)	298300 (16400–421400)	6866 (0–20000)		2096 (1500–4300)	162 (3–448)		51 (0–134)	19.63 (0–49.4)	11 (1.8–49)	4 (0–65)	5 (0–27)	0.05 (0–1.1)	Abu-Zied and Hariri (2016)
Jeddah Coast					8506			479		623	246	252	363			Al-Mur et al. (2017)
Southern Corniche, Jeddah					1081 (73–6706)			24 (6–129)		23 (3.9–121)	12.8 (4.9–61.7)	6 (0.5–55)	4 (0–21)	21 (17–29)	0.1 (0–0.7)	Abu-Zied et al. (2016)
Red Sea Coast (Jeddah)					2032–2671			34–205		52–76	12.98–22.81	17–24	80–99	68–86	3.1–3.5	Badr et al. (2009)

Table 2 (continued)

| Location	Al	Mg	Ca	Fe	Sr	K	Mn	Li	Zn	Cr	Cu	Pb	Ni	Cd	Reference
Worldwide and mangrove sediments:															
Red Sea	3742			4912	3844		83.1		20.2	44.8	7.53	1.79	20.1	0.34	Alma-hasheer et al. 2018
Zhanjiang Bay, China				38280			420		73.6	63.8	18.7	43.9	22.4	0.15	Zhang et al. (2018)
Arabian Gulf, mangrove sediments:									48.48	49.18	43.06	26.61	22.88	3.21	Alsa-madany et al. (2020)
Sundarban, Bangladesh, mangrove sediments	12200			42172			741		74.1	52.9	44.7	25.6	207	0.09	Kumar et al. (2016)
Brazil, mangrove sediments				41600					483	42.4	98.6	161		1.32	Kehrig et al. (2003)
Queensland, Australia	5380–14732			1056–117192			103		23–56	7–72	1–12	36	9	0.6	Preda and Cox (2002)
Hong Kong (Lantau Island, THW)				48100			340		152	24.5	45.6	91	46.3	1.19	Tam and Wong (2000)
Colombia (Cienaga Grande)				15593			623		91	13.2	23.3	12.6	32.5	1.92	Perdomo et al. (1999)
World average shale	80000	15000	16000	47200	300	266200	850	66	95	90	45	20	50	0.3	Turekian and Wedepohle (1961)
Sediment quality guidelines (SQGs):															
Effect range low (ERL)									150	81	34	46.7	20.9	1.2	Long et al. (1995)
Effect range median (ERM)									410	370	270	218	51.6	9.6	Long et al. (1995)
Threshold effect level (TEL)									123	37.3	35.7	35	18	0.6	MacDonald et al. (2000)
Probable effect level (PEL)									315	90	197	91.3	36	3.53	MacDonald et al. (2000)
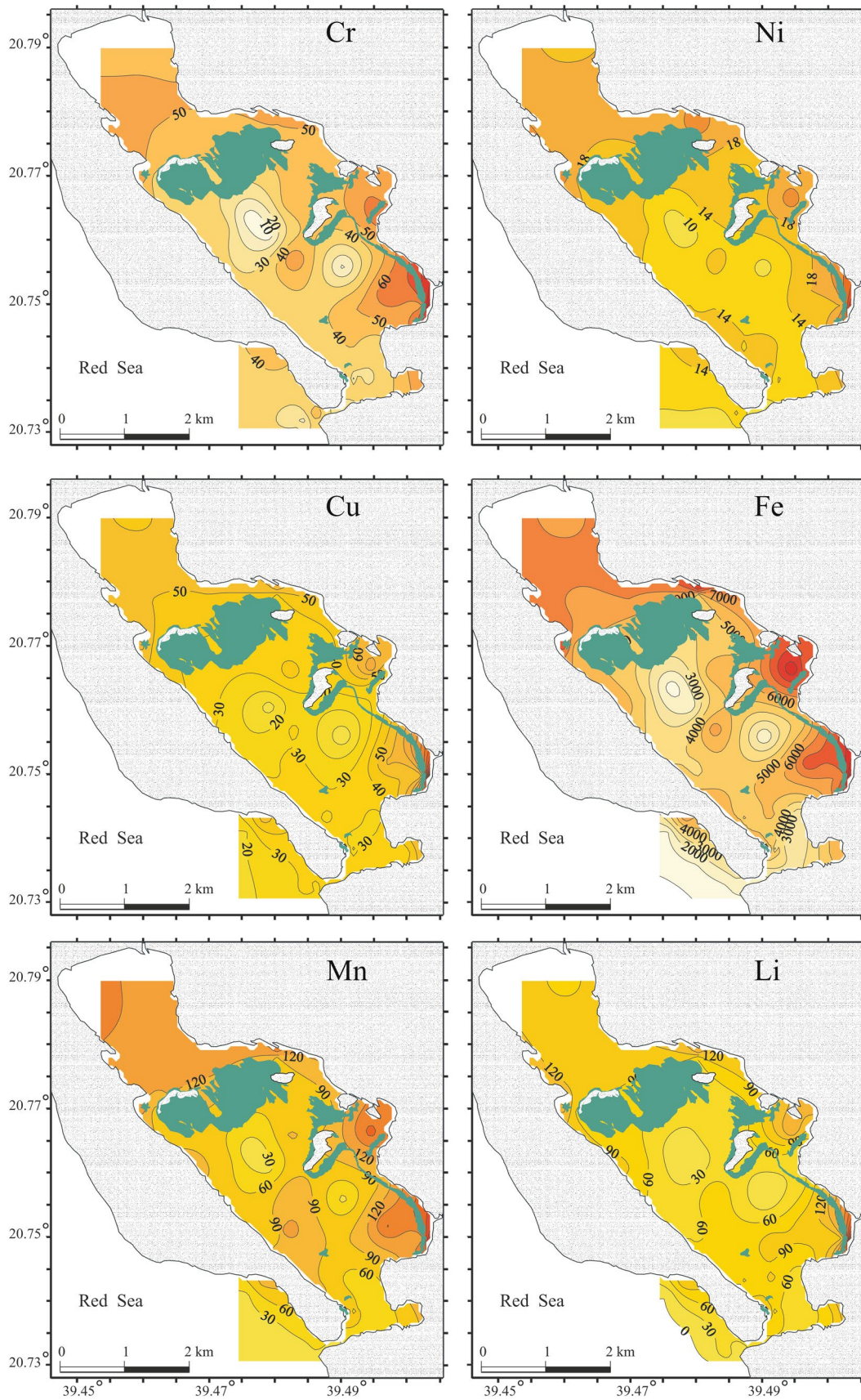
Fig. 4 Concentration (mg/kg) distribution of the metals Cr, Ni, Cu, Fe, Mn and Li in the surficial bottom sediments of Al-Shuaiba Lagoon
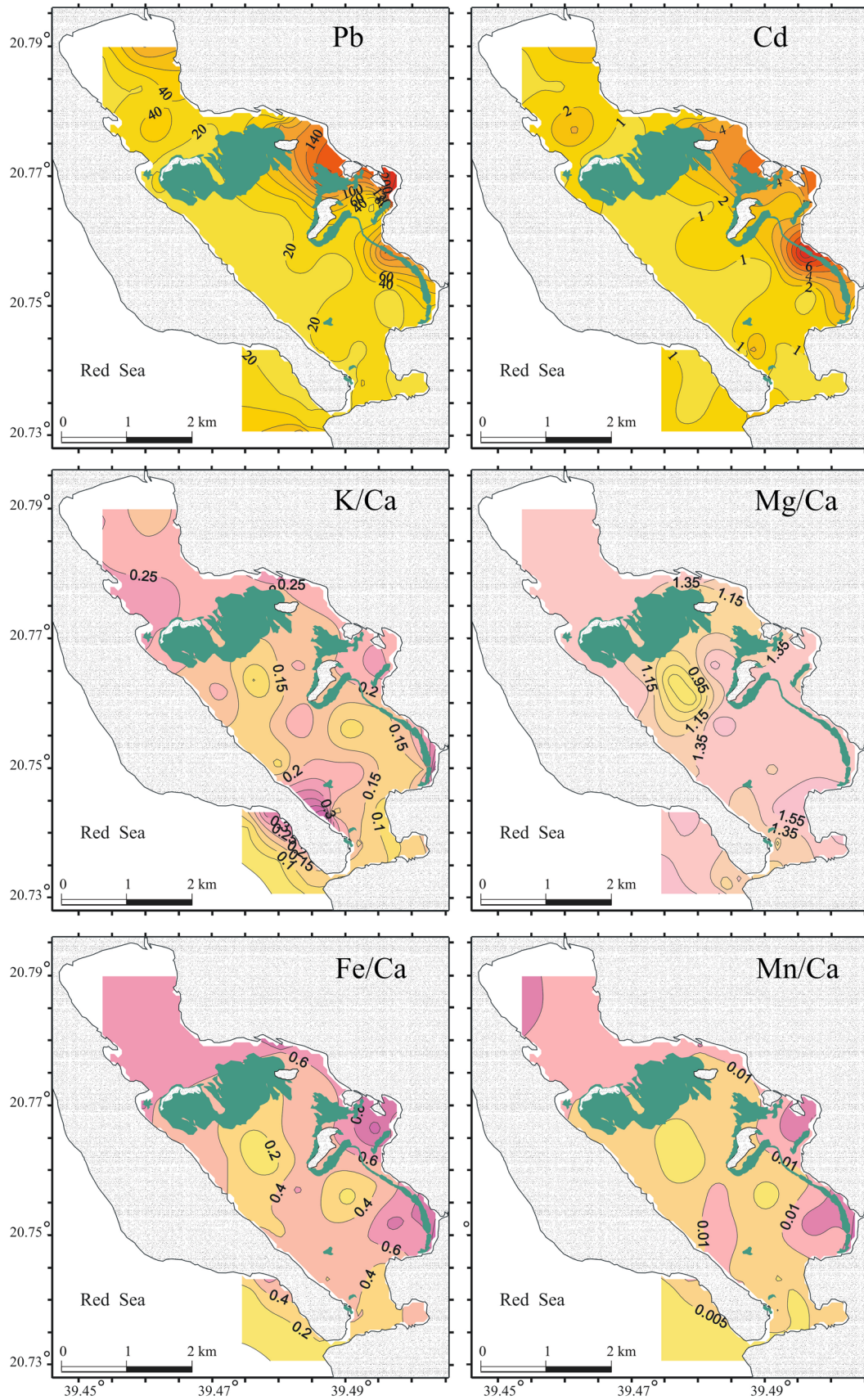
◄**Fig. 5** Concentration distribution of the metals Pb and Cd (mg/kg) and elemental ratios of K/Ca, Mg/Ca, Fe/Ca and Mn/Ca in the surficial bottom sediments of Al-Shuaiba Lagoon

where the supra-, and inter-tidal areas are more spacious with high plant cover, such as mangroves, macro-algae and seagrasses (Abu-Zied et al. 2011). In the plot of PCA, they are positively inter-correlated but with no affinity to environmental parameters, such as pH, sand, mud and water depth and other elements, such as Ca, Mg and Sr (Fig. 2). They are inversely correlated with the DO and more or less directly correlated with LOI, gravel, surface temperature and salinity; and they are strongly correlated with Fe, Mn, and Li (Fig. 2). These correlations are also indicated by the Pearson's correlation matrix (Table 1).

All elements of the association Al-Zn-Cr-Ni-Cu showed their low values in the centre of the ASL and inlet sediments, except Zn that remarkably increased to > 60 mg/kg in the inlet sediments (Figs. 3 and 4). The increase of Zn in the inlet sediments could be likely related to boat activities, such as decay of boat painting and oil spills at the boatyard area, which is located at inner inlet. Another explanation for the increase of Zn in the inlet could be naturally occurring due to biosorption by mucus algae that proliferate on coral debris and coarse grains of the inlet's sediments (Hariri and Abu-Zied 2018).

Occurrence of Al (major element) with the minor elements Zn, Cr, Ni and Cu in one association may indicate that they originated from the same sources, such as wind-blown dust enriched in aluminosilicate minerals (Basaham et al. 2019), runoff from the surrounding low-land during the rainy seasons and in-wash of sediments by tidal currents, that run over for > 5 km on the low-land in the eastern side of the lagoon. A similar association (Al-Zn-Cr-Cu) was also recorded in a short sediment core recovered from shallow waters off Jeddah City (Badr et al. 2009). The elements Zn, Ni and Cu showed pronounced concentrations in the northern and eastern sides of the lagoon where mangroves, seagrasses and macro-algae proliferate, which may act as bio-accumulator and sinks for heavy metals (Lacerda et al. 1993; Tam and Wong 2000; Almahasheer et al. 2018). These vegetations absorb nutrients and elements from the surface and underlying layers of the lagoon's sediments. When their leaves or branches shed, they fall to the bottom of the lake and decompose, returning the elements back to the bottom sediments. With this process going for a long period of time, these elements accumulate in mangrove's sediments and lead to increase the organic matter contents, which in turn also attract and store the elements due to their strong adsorption capacity (Lacerda et al. 1993; Tam and Wong 2000; Abu-Zied et al. 2013). Also, Mercone et al. (2001) indicated that the organic carbon is responsible for the elevated values of Cu,

Cr, Ni and Zn in the organic-rich sediments (sapropel S1) of core LC-21 retrieved from the eastern Mediterranean.

The association Fe–Mn-Li: It showed concentrations with averages of 4899 ± 2939, 91 ± 56 and 79 ± 75 mg/kg of bulk sediments, respectively (Fig. 4). The distributional patterns of Fe, Mn and Li are similar, suggesting same sources and displaying their maximum values in the northern and eastern sides of the lagoon where the supra-, and inter-tidal areas are more spacious with high plant cover, such as mangroves, macro-algae and seagrasses; their low values were recorded in the centre of the ASL and inlet sediments (Fig. 4). This association showed no affinity to the environmental parameters, such as DO, surface temperature, salinity, water depth, LOI and sediment grain sizes, as indicated by the plot of FA (Fig. 2). In the plot of the PCA, the association Fe–Mn-Li is positively correlated with the association Al-Zn-Cr-Ni-Cu, and weakly correlated with the LOI (Fig. 2). These correlations are also in agreement with the Pearson's correlation values where the Fe and Mn are strongly positively correlated, $r = 0.95$ (Table 1).

The association Fe–Mn with Li may indicate that they could have originated from same source. Their sources in the ASL's sediments could possibly come mainly from wind-blown dust, runoff and uptake from lagoon's water by aid of organic carbon (Thomson et al. 2001). Fe and Mn are very similar in their biogeochemistries, and mainly present in seawaters as oxyhydroxides and particulate phases, which have a great potential for scavenging of many trace elements (Raiswell et al. 2006; Raiswell and Canfield 2012; Wehrmann et al. 2014). However, the Fe is more sensitive to oxidation than Mn. In the Vistula Lagoon (Baltic Sea) metal–organic complexes contributed up to 20% of the total manganese flux and up to 70% of the total iron flux (Pakhomova et al. 2007).

The Fe and Mn concentrations in marine sediments are influenced by the redox potential, where under reducing conditions, Fe^{2+} and Mn^{2+} become soluble and release from the sediments; and under oxidizing conditions these ions leave the overlying water to be deposited on the sea floor (Mercone et al. 2001; Pakhomova et al. 2007; Abu-Zied et al. 2013; Wehrmann et al. 2014). In the ASL, these ions did not show a special response to the organic-rich substrates of the mangroves' environment, but instead they showed the highest concentrations in the supra-, and inter-tidal areas whether with organic-rich substrates or not (Fig. 4). This may suggest that the upper 1–2 cm of the organic-rich substrates of the mangroves is oxic and the redox-cline occurs below this. This might limit the recycling of Fe and Mn to the overlying intertidal waters. Pakhomova et al. (2007) concluded that organically complexed Fe and Mn were in most cases not involved in the benthic exchange processes. Also, the mangroves' environment is characterized by low water dynamics so many authors have considered it as a

trap for fine particles, which is the main sink for heavy metals (Lacerda et al. 1993; Tam and Wong 2000; Alsamadany et al. 2020).

The association Pb–Cd: It showed concentrations with averages of 37 ± 49 and 1.6 ± 2 mg/kg of bulk sediments, respectively (Fig. 5). The distributional patterns of Pb and Cd are similar, suggesting same sources and possibly same recycling under the environmental conditions of the ASL. They displayed their maximum values in the sediments of eastern side (rich in mangroves, macro-algae and seagrasses) of the lagoon whereas in the rest of lagoon and inlet, the Pb and Cd concentrations are nearly absent (Fig. 5). This association showed no affinity to the rest of studied elements and environmental parameters, such as pH, DO, surface temperature, salinity, water depth, LOI and sediment grain sizes, as indicated by the plot of FA (Fig. 2). This is in agreement to those of the Pearson's correlation values, except Pb showed strong positive correlation ($r = 0.88$) with the DO (Table 1). A similar association (Pb–Cd) was also recorded in a short sediment core recovered from shallow waters off Jeddah City (Badr et al. 2009). In the plot of the PCA, the Pb and Cd are positively correlated with mud, salinity and Ca; they are strongly inversely correlated with pH, sand, water depth, Sr and Mg (Fig. 2), indicating the effect of redox conditions on their concentrations in the sediments.

The Pb and Cd are non-essential metals and not required by micro-organisms, but they are toxic and can be accumulated in living organisms, causing various diseases and disorders even at relatively low concentrations (Rubio-Franchini et al. 2008; Pehlivan et al. 2009; Tangahu et al. 2011). Their sources in the ASL sediments could have come from atmospheric fallout (Frignani et al. 1997; Nagajyoti et al. 2010; Basaham et al. 2019), runoff and uptake from lagoon's water by aid of organic carbon. The highly elevated Pb and Cd in the organic-rich substrates of the mangroves indicate that the abundance of organic matter in the bottom sediments of the lagoon creates an environment with a high demand for oxygen, especially during summer when the degradation of the organic matters intensified. It is known that the mangrove sediments are anaerobic and reduced, rich in sulphide and organic matter content, thus favouring the retention of the water-borne heavy metals (Lacerda et al. 1993; Tam and Wong 2000). Under post-oxic and anoxic conditions, Cd gets fixed in sediments forming an insoluble species with trace sulphide, whereas in oxic conditions, it decreases in the sediments due to its release in the overlying waters as soluble species (Thomson et al. 2001). Thus, it is likely that occurrence of organic complexes and limited dissolved oxygen in the substrates of the mangrove trees allowed the retention of more Pb and Cd in eastern side of the ASL, where organic matters could create a complexing reaction, and decreases the metallic bioavailability. Little is known about the behavior of Pb at the redox-cline. However, after high

turbidity and aeration of bottom sediments, the released Pb and Cu were almost totally scavenged in the 4 h by the newly precipitated Fe oxyhydroxides, while more than 50% of the mobilized Cd remained in the dissolved fraction (Caetano et al. 2003). Also, Spencer et al. (2003) concluded that Pb (and Cu and Zn) commonly co-precipitates with sulphides below the redox-cline and therefore may show enrichment at depth.

Elemental ratios

In this study, the minor/trace elements are normalized against the major elements, such as Al, Ca and Mg, to shed light on source of elements and their geochemical processes, such as mineralization and redox conditions. Al is mainly originated from aluminosilicate detritus, while elevated values of Ca and Mg are indication of high salinity seawaters. It was mentioned that element/Al ratios reflect source characteristic as well as weathering and transportation (Piper and Calvert 2011).

The distribution patterns of Ca normalized K, Mg, Fe, Mn in the ASL's surficial sediments showed some anomalies though not much prominent (Fig. 5). The K/Ca ratio in the ASL's surficial sediments was 0.15 in the inlet and centre of the ASL, and increased to 0.25 in the northern and eastern sides (Fig. 5). The Mg/Ca ratio in the ASL's surficial sediments was 1.4 throughout the lagoon; and towards centre, it showed the lowest value of 0.6 (Fig. 5). The ratios of Fe/Ca and Mn/Ca, which are considered as potential proxies for redox conditions (Glock et al. 2012) and terrigenous inputs (Mulitza et al. 2007) are low, displaying values of 0.4–0.6 and 0.01, respectively (Fig. 5). The recorded low values of the above-mentioned elemental ratios indicate the predominance of marine biogenic carbonate mineralization in the lagoon and restricted delivery of terrigenous sediment into the lagoon. Meanwhile, Jennerjahn et al. (2004) reported that the remarkable increase of Fe/Ca ratio indicates a shift from carbonate to lithogenic deposition.

The distribution patterns of Sr/Ca and Sr/Mg ratios in the ASL's surficial sediments displayed the lowest values (0.2 and 0.22, respectively) in the centre of the lagoon, whereas the highest values (0.44 and 0.28, respectively) occurred in the supra-, and inter-tidal areas of the lagoon (Fig. 6). This indicates that much more Sr-rich calcite (aragonite) was precipitated in the intertidal areas than in the deeper part of the lagoon. The intertidal areas (without mangrove trees) of the ASL are characterized by having shallow, agitated waters with high temperature and salinity (Abu-Zied et al. 2011). Also, the Al/Ca ratio showed the lowest values (1.0) in the centre of the lagoon, whereas the highest values (4.0) occurred in the intertidal area (Fig. 6).

On the other hand, the distribution patterns of Al normalized Ca, Mg, Fe, K, Zn, Cu and Ni increased in the middle
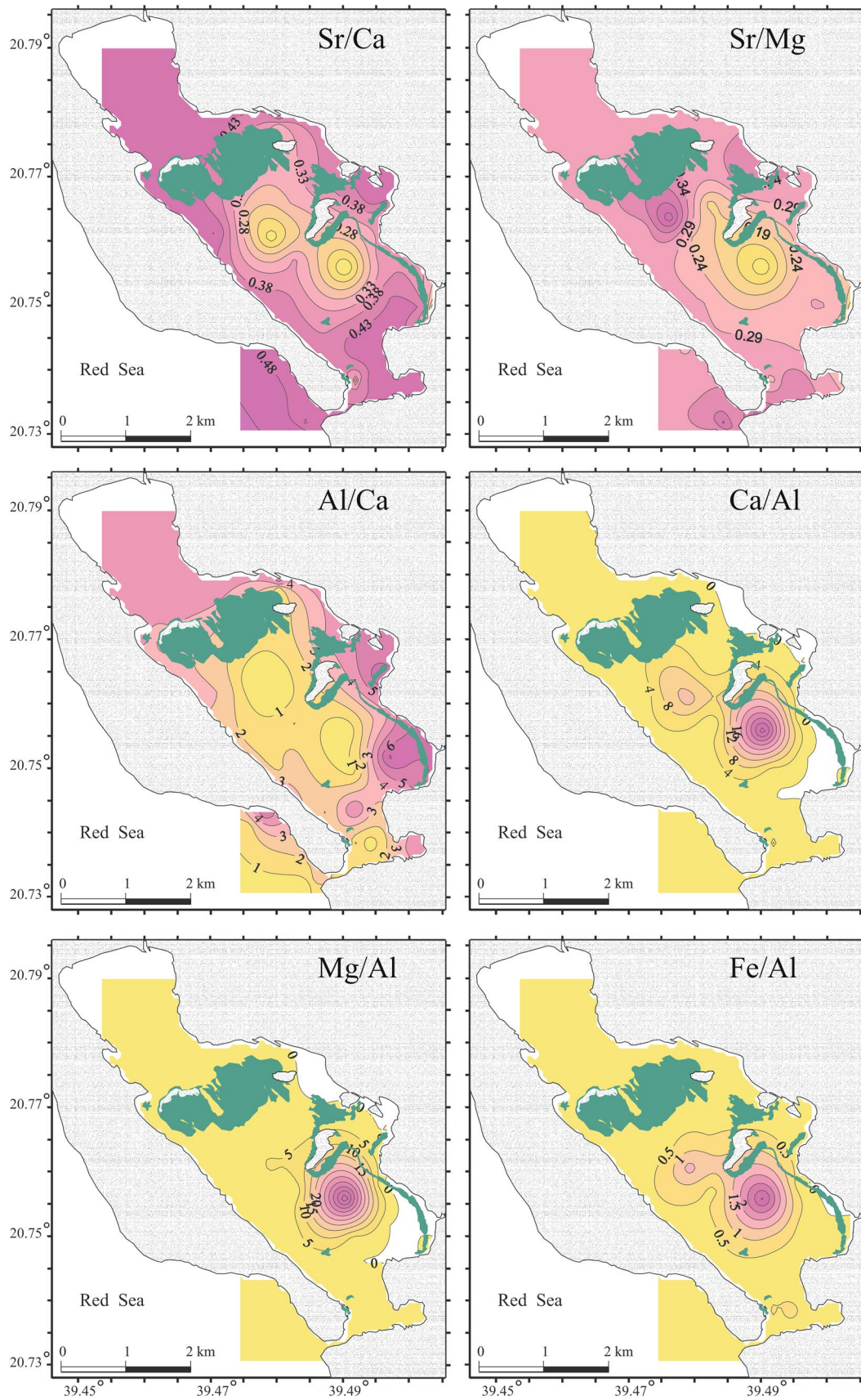
Fig. 6 Distribution of the elemental ratios of Sr/Ca, Sr/Mg, Al/Ca, Ca/Al, Mg/Al and Fe/Al in the surficial bottom sediments of Al-Shuaiba Lagoon
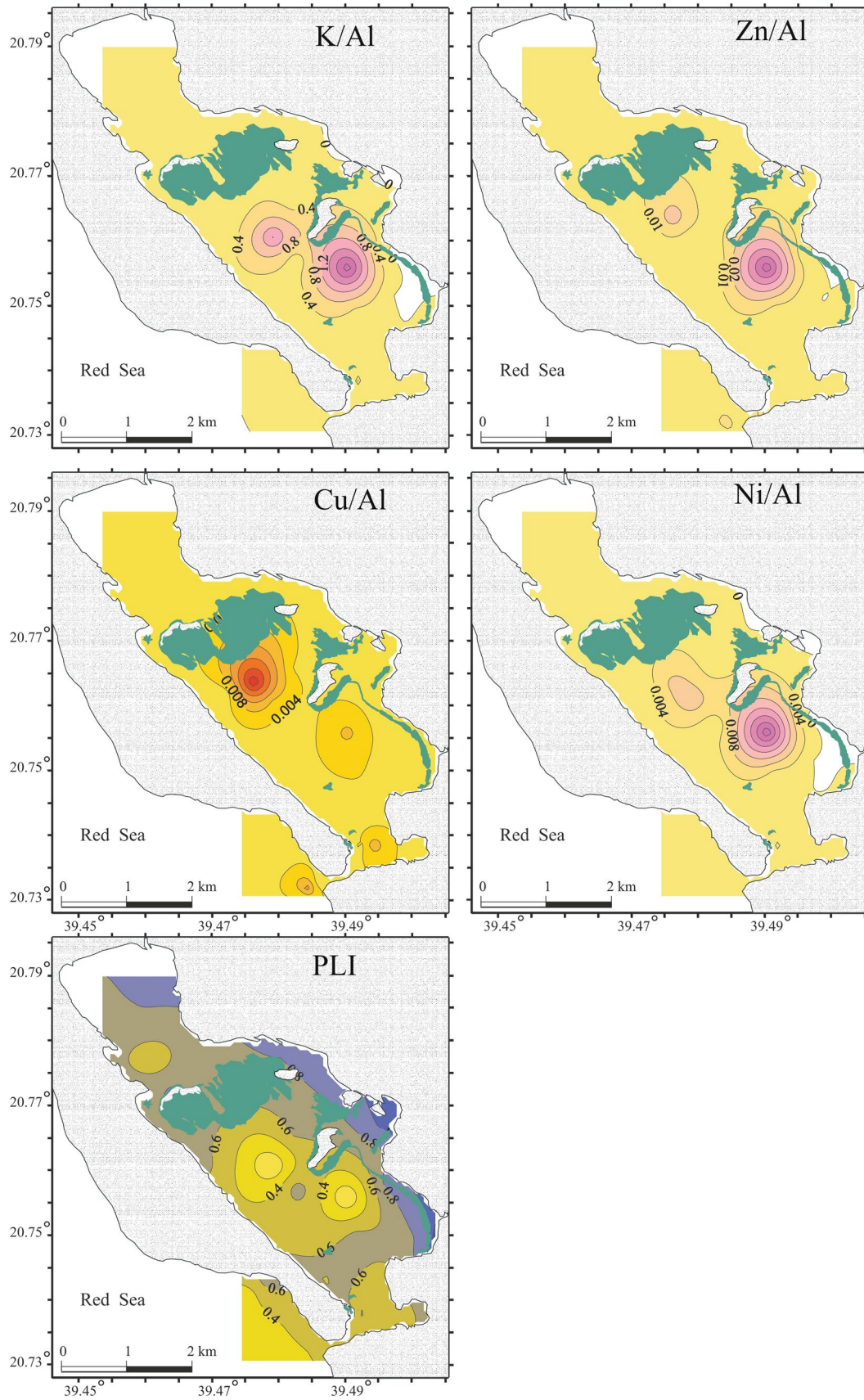
◀**Fig. 7** Distribution of the elemental ratios of K/Al, Zn/Al, Cu/Al and Ni/Al, and the pollution load index (PLI) values in the surficial bottom sediments of Al-Shuaiba Lagoon

of the lagoon displaying values of > 10, > 10, 0.8, 1.2, 0.04, 0.01 and 0.01, respectively (Figs. 6 and 7). In the intertidal area of the lagoon, they were absent (Figs. 6 and 7). This may indicate that the bottom sediments of the lagoon's centre are enriched by Mg-calcite, which may be incorporated or coated with cations, such as of Fe, K, Zn, Cu and Ni.

Metal enrichment in the ASL's sediments

The enrichment of metals in the surficial sediments of the ASL was explored by many indices (EF, CF, Igeo and PLI), which all were compared against the world average shale (Turekian and Wedepohl 1961) and normalized by Al. In this study, the metals' enrichment (if present) is attributed to natural sources since the ASL is safe, at the moment, from any anthropogenic activities, except there is a little fishing activities at the inlet. It is far from the urbanization activities of Jeddah City by about 80 km.

The EFs of Fe, K and Mn were < 1.0, indicating the enrichments of these metals in the surficial sediments of the ASL were very low and did not exceed the world shale (Table 2). The metals Cr, Zn, Cu, Ni and Li showed enrichments between 2 and 5 that means they were in moderate enrichments, whereas the metals Mg, Ca and Pb were significantly enriched with values of 11, 8 and 13 (respectively), when comparing with the world shale (Table 2). The metals that showed EFs > 2 is possibly related to natural sources (as discussed above), such as mineralization of lagoon's water, wind-blown dust, runoff and then uptake/concentration by the fine particles and organic matters. The metals Sr and Cd were extremely high enriched in the bottom sediments of the ASL, showing values of 103 and 43, respectively (Table 2). This is because the lagoon has hypersaline waters with restricted water exchange and is located under warm tropical climate favouring the deposition of Sr-rich carbonates (aragonite). The enrichment of Cd is attributed to concentration in sediments by the uptake of organic complexes, likely, in suboxic to anoxic environments.

The CFs of metals, such as Al, Fe, Mg, Ca, K, Mn, Cr, Zn, Cu and Ni, were < 1.0 (Table 2), indicating the bottom sediments of the ASL were not contaminated by these metals, which showed average concentrations less than the world shale. The ASL's sediments were moderately contaminated by Pb and Li, which showed CFs of 1.8 and 1.2, respectively (Table 2). They were considerably contaminated by Cd (CF = 5.3); and very highly contaminated by Sr (CF = 13.3) (Table 2). The contamination of the ASL bottom sediments especially of the mangrove substrates with Pb and Cd may induce an adverse effect on the living biota since they are

known as toxic metals. This may be one of the common cause for occurrence of many dead, dwarfed and senescent mangrove trees at the eastern side of the ASL, where accumulations of heavy metals can cause direct and/or indirect reduction of plant growth by adversely affecting various physiological and molecular activities of plants (Tiwari and Lata 2018).

Based on the values of the Igeo of all metals (Igeo < 0.0) indicated that the surficial sediments of the ASL were unpolluted, but they were unpolluted to moderately polluted by Sr and Cd, which showed Igeo of 0.92 and 0.32, respectively (Table 2). However, Sr is a major, non-toxic, macro-element, essential for calcium carbonate production.

The PLI of the essential metals (Fe, Mn, Cr, Zn, Cu, and Ni) and toxic metals (Pb and Cd) showed an average value of < 1.0 throughout the whole lagoon, except the samples SH27 and SH29, located in the eastern side, their PLIs exceeded 1.0 (Fig. 7). This indicated that the surficial sediments of the ASL were unpolluted, but at the eastern side it likely became naturally polluted.

Comparison with the regional Red Sea, worldwide and SQGs

Comparing the concentrations of the studied essential metals (Fe, Mn, Zn, Cr, Cu, and Ni) and toxic metals (Pb and Cd) in the ASL with other localities in the Red Sea, worldwide and sediment quality guidelines (SQGs) (Table 2) helps to know to what extent these concentrations are similar with the other studies and whether they have an adverse impact on the living organisms in the lagoon or not. Also, the toxicity of metal or bioavailability cannot determined by the metal concentration itself, but it should be compared with one of the commonly used SQGs such as those of Long et al. (1995) and MacDonald et al. (2000).

In general, the concentrations of Fe, Mn, Zn, Cr, Cu, and Ni in the surficial sediments of the ASL appear to be within their natural range, showing values smaller than the world shale, while the concentrations of Pb and Cd were higher than the world shale (Table 2). The Fe and Mn showed values more or less similar to those of the Red Sea coast. But, these values were lower than those of the Red Sea lagoons, such as Al-Kharrar, Sharm Obhur, Al-Arbaeen and Al-Shabab (Table 2). This is due to their connection with lithogenic influxes from wadies and sewage influents, but the ASL has no connection to any of these. Also, they were smaller than those of the world mangrove sediments (Table 2).

The concentrations of Cr, Zn, Cu, and Ni were more or less similar to those of the Red Sea lagoons except Sharm Obhur, Al-Arbaeen and Al-Shabab lagoons, which contained higher concentrations of these metals due to pollution sources from the municipality of Jeddah City (Abu-Zied

et al. 2013; Ghandour et al. 2014). They showed values more or less similar to those of the Red Sea coast, except the higher values recorded by Al-Mur et al. (2107) that was related to occurrence of pollution sources (Table 2). Also, they showed similar concentrations to those of the world mangrove sediments (Table 2).

The concentrations of Pb and Cd were higher than those of the Red Sea lagoons and world shale, but they were more or less similar to the higher values of the polluted lagoons, such as the Al-Arbaeen and Al-Shabab lagoons (Table 2). Also, they were higher than those of the Red Sea coast, but they were similar to those of the polluted sediments investigated by Badr et al. (2009) and Al-Mur et al. (2017). Also, they were more or less similar to those of the world mangrove sediments (Table 2).

When comparing the concentrations of Zn, Cr, Cu, Ni, Pb and Cd in the ASL sediments with the SQGs (Table 2), it is noted that the concentrations of Zn and Ni are lower than the effect range low (ERL) of NOAA (Long et al. 1995) and threshold effect level (TEL) (MacDonald et al. 2000). This suggests that the present concentrations of these metals in the ASL are not associated with adverse impacts on the living organisms in the ASL. The concentration of Cr showed similar conditions to that of Zn and Ni, but it is slightly higher than the TEL, suggesting that it may cause an occasional threat to the biology of the lagoon.

The concentrations of Cu, Pb and Cd in the ASL sediments are higher than the values of ERL and TEL and lower than the values of effect range median (ERM) of NOAA (Long et al. 1995) and probable effect level (PEL) (MacDonald et al. 2000) (Table 2). This suggests that these metals could cause an occasional threat to the biota of the lagoon.

Conclusion

The concentrations of major (Al, Mg, Ca, Sr and K) and trace metals (Fe, Mn, Li, Zn, Cr, Cu, Pb, Ni and Cd) in the surficial bulk sediments (dry wt) of the ASL were measured. Their enrichment based on comparison with the natural background shale and normalizing with Al decreased in the following order: Sr, Cd, Pb, Mg, Ca, Cu, Li, Zn, Cr, Ni, K, Mn and Fe. All metal spatial distributions indicated that the elevated concentrations occurred in the intertidal areas and in the mangrove sediments and decreased in a gradient towards the deep waters and inlet, except Ca, which showed elevated concentration in the centre of the lagoon.

The statistical analyses allowed the division of measured elements into five associations. The major metal Mg-Ca-Sr and K associations showed a close affinity to pH, temperature, salinity and dissolved oxygen (DO) as indicated by the FA, suggesting they could have mainly originated from the lagoon's water mineralization due to evaporation concentration processes and precipitation of biogenic and non-skeletal carbonates. The associations Al-Zn-Cr-Ni-Cu and Fe–Mn-Li showed positive inter-relationships and direct correlations with organic carbon (LOI) as indicated by the PCA, suggesting that the main sources of them were mainly from wind-blown dust and runoff from the surrounding lowland, enriched in aluminosilicate minerals, during the rainy seasons and in-wash of sediments by tidal currents. The Pb–Cd association showed strong inverse relationship with the pH (PCA plot) indicating the effect of redox conditions on their concentrations in the sediments. Elevated values of Pb–Cd were exclusively found in the mangrove sediments, implying that the occurrence of organic complexes and limited dissolved oxygen in the substrates of the mangrove trees allowed the retention of more Pb and Cd in the eastern side of the ASL, where the mangroves predominate.

The CF, Igeo and PLI values indicated that the bottom sediments of the ASL contain safe concentrations of Al, Fe, Mg, Ca, K, Mn, Cr, Zn and Ni, but they were polluted by Cu, Pb and Cd due to natural processes. This is also deduced by the SQGs where the concentrations of Cu, Pb and Cd are higher than the values of ERL and TEL and lower than the values of ERM, suggesting that these metals could cause an occasional threat to the living biota, especially at the eastern side of the lagoon.

References

Abohassan RA (2013) Heavy metal pollution in avicennia marina mangrove systems on the Red Sea Coast of Saudi Arabia. JKAU 24:35–53

Abu-Zied RH, Bantan RA (2013) Hypersaline benthic foraminifera: their environmental controls and usefulness in sea level reconstruction at the Shuaiba Lagoon, Eastern Red Sea, Saudi Arabia. Mar Micropaleontol 103:51–67

Abu-Zied RH, Bantan RA (2015) Palaeoenvironment, palaeoclimate and sea-level changes in the Shuaiba Lagoon during the late Holocene (last 3.6 kyr), Eastern Red Sea Coast. Saudi Arabia the Holocene 25:1301–1312

Abu-Zied RH, Hariri MS (2016) Geochemistry and benthic foraminifera of the nearshore sediments from Yanbu to Al-Lith, eastern Red Sea Coast. Saudi Arabia Arab J Geosci 9:245. https://doi.org/10.1007/s12517-015-2274-9

Abu-Zied RH, Orif MI (2019) Recent environmental changes of Al-Salam Lagoon as inferred from core sediment geochemistry and

benthic foraminifera, Jeddah City. Saudi Arabia Environ Earth Sci 78:60. https://doi.org/10.1007/s12665-019-8057-y

Abu-Zied RH, Bantan RA, El Mamoney MH (2011) Modern environmental conditions and macro-fauna and flora characteristics of Shuaiba Lagoon, Red Sea Coast. Saudi Arabia JKAU: Mar Sci 22:159–179

Abu-Zied RH, Basaham AS, El Sayed MA (2013) Effect of municipal wastewaters on bottom sediment geochemistry and benthic foraminifera of two Red Sea coastal inlets, Jeddah, Saudi Arabia. Environ Earth Sci 68:451–469

Abu-Zied RH, Al-Dubai TAM, Bantan RA (2016) Environmental conditions of shallow waters alongside the southern Corniche of Jeddah based on benthic foraminifera, physico-chemical parameters and heavy metals. J Foram Res 46:149–170

Almahasheer H, Serrano O, Duarte CM, Irigoien X (2018) Remobilization of heavy metals by mangrove leaves. Front Mar Sci 5:484. https://doi.org/10.3389/fmars.2018.00484

Al-Mur BA, Quicksall AN, Al-Ansari AMA (2017) Spatial and temporal distribution of heavy metals in coastal core sediments from the Red Sea, Saudi Arabia. Oceanologia 59:262–270

Alsamadany H, Al-Zahrani HS, Selim EM, El-Sherbiny MM (2020) Spatial distribution and potential ecological risk assessment of some trace elements in sediments and grey mangrove (*Avicennia marina*) along the Arabian Gulf coast, Saudi Arabia. Open Chem 18:77–96

Amir M, Paul D, Samal RN (2019) Sources of organic matter in Chilika lagoon, India inferred from stable C and N isotopic compositions of particulates and sediments. J Mar Syst 194:81–90

Amir M, Paul D, Malik JN (2020) Geochemistry of Holocene sediments from Chilika Lagoon, India: inferences on the sources of organic matter and variability of the Indian summer monsoon. Quatern Int. https://doi.org/10.1016/j.quaint.2020.08.050

Badr NBE, El-Fiky AA, Mostafa AR, Al-Mur BA (2009) Metal pollution records in core sediments of some Red Sea coastal areas, Kingdom of Saudi Arabia. Environ Monit Assess 155:509–526

Bantan RA, Abu-Zied RH (2014) Sediment characteristics and molluscan fossils of the Farasan Islands shorelines, southern Red Sea, Saudi Arabia. Arab J Geosci 7:773–787

Basaham AS, El Sayed MA, Ghandour IM, Masuda H (2015) Geochemical background for the Saudi Red Sea coastal systems and its implication for future environmental monitoring and assessment. Environ Earth Sci 74:4561–4570

Basaham AS, Ghandour IM, Haredy R (2019) Controlling factors on the geochemistry of Al-Shuaiba and Al-Mejarma coastal lagoons, Red Sea, Saudi Arabia. Open Geosci 11:426–439

Caetano M, Madureira M, Vale C (2003) Metal Remobilisation during resuspension of anoxic contaminated sediment: short-term laboratory study. Water Air Soil Pollut 143:23–40. https://doi.org/10.1023/A:1022877120813

Chakravarty M, Patgiri AD (2009) Metal pollution assessments of Dikrong River, N.E. India J Hum Ecol 27:63–67

Clemente R, Dickinson NM, Lepp NW (2008) Mobility of metals and metalloids in a multi-element contaminated soil 20 years after cessation of the pollution source activity. Environ Pollut 155:254–261

Diop C, Dewaelé D, Cazier F, Diouf A, Ouddane B (2015) Assessment of trace metals contamination level, bioavailability and toxicity in sediments from Dakar coast and Saint Louis estuary in Senegal, West Africa. Chemosphere 138:980–987

Esmaeilzadeh M, Karbassi A, Moattar F (2016) Heavy metals in sediments and their bioaccumulation in Phragmites australis in the Anzali wetland of Iran. Chin J Oceanol Limnol 34:810–820

Frignani M, Belluci LG, Langone L, Muntau H (1997) Metal fluxes to the sediments of the northern Venice lagoon. Mar Chem 58:275–292

Garcia CAB, Barreto MS, Passos EA, Alves JPH (2009) Regional geochemical baselines and controlling factors for trace metals in

sediments from the Poxim River. Northeast Brazil J Braz Chem Soc 20:1334–1342

Ghandour IM, Basaham S, Al-Washmi A, Masuda H (2014) Natural and anthropogenic controls on sediment composition of an arid coastal environment: Sharm Obhur, Red Sea, Saudi Arabia. Environ Monit Asses 186:1465–1484

Glock N, Eisenhauer A, Liebetrau V, Wiedenbeck M, Hensen C, Nehrke G (2012) EMP and SIMS studies on Mn/Ca and Fe/Ca systematics in benthic foraminifera from the Peruvian OMZ: a contribution to the identification of potential redox proxies and the impact of cleaning protocols. Biogeosciences 9:341–359. https://doi.org/10.5194/bg-9-341-2012

Gussone N, Zonneveld K, Kuhnert H (2010) Minor element and Ca isotope composition of calcareous dinoflagellate cysts of cultured *Thoracosphaera heimii*. Earth Planet Sci Lett 289:180–188

Hakanson L (1980) An ecological risk index for aquatic pollution control. A Sedimentological Approach Wat Res 14:975–1001

Hammer Ø, Harper DAT, Ryan PD (2001) Past: paleontological statistics software package for education and data analysis. Palaeontol Electron 4:1–9

Hariri MSB, Abu-Zied RH (2018) Factors influencing heavy metal concentrations in the bottom sediments of the Al-Kharrar Lagoon and Salman Bay, eastern Red Sea coast. Saudi Arabia Arab J Geosci 11:495. https://doi.org/10.1007/s12517-018-3838-2

Hu J, Lin B, Yuan M, Lao Z, Wu K, Zeng Y, Liang Z, Li H, Li Y, Zhu D, Liu J, Fan H (2019) Trace metal pollution and ecological risk assessment in agricultural soil in Dexing Pb/Zn mining area, China. Environ Geochem Health 41:967–980. https://doi.org/10.1007/s10653-018-0193-x

Jennerjahn TC, Ittekkot V, Arz HW, Behling H, Pätzold J, Wefer G (2004) Asynchronous terrestrial and marine signals of climate change during Heinrich events. Science 306:2236–2239

Kumar A, Ramanathan A, Prasad MB, Datta D, Kumar M, Sappal SM (2016a) Distribution, enrichment, and potential toxicity of trace metals in the surface sediments of Sundarban mangrove ecosystem, Bangladesh: a baseline study before Sundarban oil spill of December, 2014. Environ Sci Pollut Res 23:8985–8999

Kumar D, Singh DP, Barman SC, Kumar N (2016b) Heavy metal and their regulation in plant system: an overview. In: Singh A, Prasad S, Singh R (eds) Plant responses to xenobiotics. Springer, Singapore, pp 19–38

Lacerda LDD, Carvalho CEV, Tanizaki KF, Ovalle ARC, Rezende CE (1993) The biogeochemistry and trace metals distribution of mangrove rhizospheres. Biotropica 25:252–257

Long ER, MacDonald DD, Smith SL, Calder FD (1995) Incidence of adverse biological effects within ranges of chemical concentrations in marine and estuarine sediments. Environ Manag 19:81–97

MacDonald DD, Ingersoll CG, Berger TA (2000) Development and evaluation of consensus-based sediment quality guidelines for freshwater ecosystems. Arch Environ Contam Toxicol 39:20–31

Martin JH, Fitzwater SE, Gordon RM (1990) Iron deficiency limits phytoplankton growth in Antarctic waters. Global Biogeochem Cycles 4:5–12

Maurya PK, Malik DS (2019) Bioaccumulation of heavy metals in tissues of selected fish species from Ganga river, India, and risk assessment for human health. Hum Ecol Risk Assess 25:905–923

Mercone D, Thomson J, Abu-Zied RH, Croudace I, Rohling EJ (2001) High-resolution geochemical and micropaleontological profiling of the most recent eastern Mediterranean sapropel. Mar Geol 177:24–44

Mulitza S, Paul A, Wefer G (2007) Late Pleistocene South Atlantic. Encyclopedia of Quaternary Science 3:1816–1831

Muller G (1969) Index of geoaccumulation in sediments of the Rhine River. GeoJournal 2:108–118

Nagajyoti PC, Lee KD, Sreekanth TVM (2010) Heavy metals, occurrence and toxicity for plants: a review. Environ Chem Lett 8:199–216

Pakhomova SV, Hall PO, Kononets MY, Rozanov AG, Tengberg A, Vershinin AV (2007) Fluxes of iron and manganese across the sediment-water interface under various redox conditions. Mar Chem 107:319–331. https://doi.org/10.1016/j.marchem.2007.06.001

Pehlivan E, Özkan AM, Dinç S, Parlayici S (2009) Adsorption of Cu_{2+} and Pb_{2+} ion on dolomite powder. J Hazard Mater 167:1044–1049

Perdomo L, Ensminger I, Fernanda Espinosa L, Elster C, Wallner-kersanach M, Schnetter ML (1999) The mangrove ecosystem of the Ciénaga Grande de Santa Marta (Colombia): Observations on regeneration and trace metals in sediment. Mar Pollut Bull 37:393–403

Piper DZ, Calvert SE (2011) Holocene and late glacial palaeoceanography and palaeolimnology of the Black Sea: changing provenance and basin hydrography over the past 25,000 years. Geochim Cosmochim Acta 75:5597–5624

Poulton SW, Raiswell R (2002) The low-temperature geochemical cycle of iron: from continental fluxes to marine sediment deposition. Am J Sci 302:774–805

Preda M, Cox ME (2002) Trace metal occurrence and distribution in sediments and mangroves, Pumicestone region, southeast Queensland, Australia. Environ Int 28:433–449

Raiswell R, Canfield DE (2012) The iron biogeochemical cycle past and present. Geochem Perspect 1:1–220. https://doi.org/10.7185/geochempersp.1.1

Raiswell R, Tranter M, Benning LG, Siegert M, De'ath R, Huybrechts P, Payne T (2006) Contributions from glacially derived sediment to the global iron (oxyhydr)oxide cycle: implications for iron delivery to the oceans. Geochim Cosmochim Acta 70:2765–2780

Ries JB (2010) Review: geological and experimental evidence for secular variation in seawater Mg/Ca (calcite-aragonite seas) and its effects on marine biological calcification. Biogeosciences 7:2795–2849

Rosales I, Robles S, Quesada S (2004) Elemental and oxygen isotope composition of early Jurassic belemnites: salinity vs. temperature signals. J Sed Res 74:342–354

Rubio-Franchini I, Mejía SJ, Rico-Martínez R (2008) Determination of lead in samples of zooplankton, water, and sediments in a Mexican reservoir: evidence for lead biomagnification? Environ Toxicol 23:459–465

Sakan S, Grzetić I, Worpević D (2006) Distribution and fractionation of heavy metals in the Tisa (Tisza) River sediments. Environ Sci Pollut Res 1–8

Sarkar SK (2018) Trace metals in a tropical mangrove wetland: chemical speciation, ecotoxicological relevance and remedial measures. Springer Nature, Singapore. https://doi.org/10.1007/978-981-10-2793-2

Simionov I-A, Cristea V, Petrea S-M, Mogodan A, Nicoara M, Baltag ES, Strungaru SA, Faggio C (2019) Bioconcentration of essential and nonessential elements in Black Sea turbot (*Psetta Maxima Maeotica* Linnaeus, 1758) in relation to fish gender. J Mar Sci Eng 7:466. https://doi.org/10.3390/jmse7120466

Souza IdC, Rocha LD, Morozesk M, Bonomo MM, Arrivabene HP, Duarte ID, Furlan LM, Monferrán MV, Mazik K, Elliott M, Matsumoto ST, Milanez CRD, Wunderlin DA, Fernandes MN (2015) Changes in bioaccumulation and translocation patterns between root and leaves of *Avicennia schaueriana* as adaptive response to different levels of metals in mangrove system. Mar Pollut Bull 94:176–184

Spencer KL, Cundy AB, Croudace IW (2003) Heavy metal distribution and early-diagenesis in salt marsh sediments from the Medway estuary, Kent, UK. Estuar Coast Shelf Sci 57:43–54

Stanienda-Pilecki KJ (2018) Magnesium calcite in Muschelkalk limestones of the Polish part of the Germanic Basin. Carbonate Evaporite 33:801–821

Sunagawa I, Takahashi Y, Imai H (2007) Strontium and aragonite-calcite precipitation. J Miner Petrol Sci 102:174–181

Sutherland RA (2000) Bed sediment-associated trace metals in an urban stream, Oahu. Hawaii Environ Geol 39:611–627. https://doi.org/10.1007/s002540050473

Tam NF, Wong YS (2000) Spatial variation of heavy metals in surface sediments of Hong Kong mangrove swamps. Environ Pollut 110:195–205

Tang J, Niedermayr A, Köhler SJ, Böhm F, Kısakürek B, Eisenhauer A, Dietzel M (2012) Sr/Ca and Ca/Ca fractionation during inorganic calcite formation: III. Impact of salinity/ionic strength. Geochim Cosmochim Acta 77:432–443. https://doi.org/10.1016/j.gca.2011.10.039

Tangahu BV, Abdullah SRS, Basri H, Idris M, Anuar N, Mukhlisin M (2011) A review on heavy metals (As, Pb, and Hg) uptake by plants through phytoremediation. Int J Chem Eng. https://doi.org/10.1155/2011/939161

Thomson J, Nixon S, Croudace IW, Pedersen TF, Brown L, Cook GT, MacKenzie AB (2001) Redox-sensitive element uptake in northeast Atlantic Ocean sediments (Benthic Boundary Layer Experiment Site). Earth Planet Sci Lett 184:535–547. https://doi.org/10.1016/S0012-821X(00)00347-2

Tiwari S, Lata C (2018) Heavy metal stress, signaling, and tolerance due to plant-associated microbes: an overview. Front Plant Sci 9:452. https://doi.org/10.3389/fpls.2018.00452

Toler SK, Hallock P, Schijf J (2001) Mg/Ca ratios in stressed foraminifera, *Amphistegina gibbosa*, from the Florida Keys. Mar Micropaleontol 43:199–206

Tripati AKML, Delaney ML, Zachos JC, Anderson LD, Kelly DC, Elderfield H (2003) Tropical sea surface temperature reconstructions for the early Paleogene using Mg/Ca ratios of planktonic foraminifera. Paleooceanography 18:1101. https://doi.org/10.1029/2003PA000937

Turekian KK, Wedepohl KH (1961) Distribution of the elements in some major units of the earth crust. Geol Soc Am Bull 72:175–192

Usman AR, Alkredaa RS, Al-Wabel M (2013) Heavy metal contamination in sediments and mangroves from the coast of Red Sea: *Avicennia marina* as potential metal bioaccumulator. Ecotoxicol Environ Safety 97:263–270

Wehrmann LM, Formolo MJ, Owens JD, Raiswell R, Ferdelman TG, Riedinger N, Lyons TW (2014) Iron and manganese speciation and cycling in glacially influenced high-latitude fjord sediments (West Spitsbergen, Svalbard): evidence for a benthic recycling-transport mechanism. Geochim Cosmochim Acta 141:628–655

Weinbauer MG, Velimirov B (1995) Calcium, magnesium and strontium concentrations in the calcite sclerites of Mediterranean gorgonians (Coelenterata: Octocorallia). Estuar Coast Shelf Sci 40:87–104

Weinbauer MG, Brandstatter F, Velimirov B (2000) On the potential use of magnesium and strontium concentrations as ecological indicators in the calcite skeleton of the red coral (*Corallium rubrum*). Mar Biol 137:801–809

Youssef M, El-Sorogy A (2016) Environmental assessment of heavy metal contamination in bottom sediments of Al-Kharrar lagoon, Rabigh, Red Sea. Saudi Arabia Arab J Geosci 9:474. https://doi.org/10.1007/s12517-016-2498-3

Zhuang P, McBride MB, Xia H, Li N, Li Z (2009) Health risk from heavy metals via consumption of food crops in the vicinity of Dabaoshan mine, South China. Sci Total Environ 407:1551–1561